Influences of Surface Properties and Impact Conditions on Adhesion of Insect Residues

Christopher J. Wohl,[1] Jereme R. Doss,[2] Michelle H. Shanahan,[2] Joseph G. Smith Jr.,[1] Ronald K. Penner[3] John W. Connell,[1] Emilie J. Siochi[1]
[1]NASA Langley Research Center, Hampton, VA 23681, United States of America
[2]National Institute of Aerospace, Hampton, VA 23666, United States of America
[3]Science and Technology Corporation, Hampton, VA 23666, United States of America

christopher.j.wohl@nasa.gov; emilie.j.siochi@nasa.gov

Introduction

Airflow over airfoils used on current commercial aircraft transitions from laminar to turbulent at relatively low chord positions.[1] As a result, drag increases, requiring more thrust to maintain flight. An airfoil with increased laminar flow would experience reduced drag and a lower fuel burn rate. One of the objectives of NASA's Environmentally Responsible Aviation project is to identify and demonstrate technologies that will enable more environmentally friendly commercial aircraft.[2] While more-aerodynamically efficient airfoil shapes can be designed, surface contamination from ice, dirt, pollen, runway debris, and insect residue can degrade performance. [1]

A number of review articles provide an overview of the approaches to mitigating insect residue adhesion.[3] Active mitigation strategies have been demonstrated to be effective, but have not been commercially implemented due to manufacturing and operational complexity, environmental impact, and weight penalties. Passive strategies, namely coatings, circumvent many of these challenges; with the emergence of superhydrophobic materials, efforts to mitigate surface contamination with coatings have increased.[4]

In previous work, it was demonstrated that both surface chemistry and surface topography influenced the ultimate residue height and areal coverage of insect residues on copolyimide and epoxy coatings.[5] In the current work, high speed photographs of fruit fly (*drosophila melanogaster*) impacts were recorded in order to visualize impact dynamics less than 0.1 s after impact. The effect of impact angle was studied on flat plates of uncoated aluminum alloy and experimental urethane and epoxy coatings were used to alter surface chemistry and topography.

Experimental

Aluminum (Al) alloy 2024-T3 clad was used as the control and also as the substrate on which experimental polymeric materials were applied. The Al 2024 control surface was cleaned prior to insect impact. The urethane and epoxy coatings discussed herein are proprietary and details regarding their composition cannot be disclosed at this time. To promote coating adhesion, Al 2024 substrates were scrubbed with an oxidative solution treated with a conversion coat, AC-131 (3M™) that populated the surfaces with amine functionalities. Epoxy coatings were applied by spraying and were cured at elevated temperature. A proprietary primer was applied prior to spray coating of the urethane and its elevated temperature cure.

Contact angle measurements were conducted using an FTA1000B goniometer (First Ten Angstroms). A minimum of three measurements using 8 µL water droplets was collected on each sample. Insect impact experiments were performed in a modified bench-top wind tunnel using flightless fruit flies (*drosophila melanogaster*) that were propelled towards the investigated surface using a custom-built pneumatic delivery device.[5a] No efforts were made to control insect age, mass, hydration, or orientation at the time of impact. On each surface, impacts of at least three intact insects were photographed at 50,000 and 100,000 frames/s. The average insect speed was determined to be ~ 66 m s^{-1} (150 mph). Insect residues were scanned using a resolution of 5 µm between data points and 20 µm between scan lines using an FRT of America optical surface profilometer (Microprof 100). Surface roughness was determined from scanned regions that did not contain residues.

Results and Discussion

Although previous work has considered insect impact events as elastic/inelastic collisions,[6] the impacts described here can be estimated as a hydrodynamic event.[7] For the high velocity impacts considered in this work, the impact pressure, which in the acoustic limit, i.e., velocity is restricted to the speed of sound, can be equated to the water hammer pressure, P_{WH},[8]

$$P_{WH} = \rho c v$$

where ρ is the fluid density, c is the speed of sound in that fluid, and v is the impact velocity. Using a haemolymph density of 1045 kg m^{-3} and a speed of sound in ethylene glycol of 1660 m s^{-1} (3710 mph),[9] the water hammer pressure/impact pressure was calculated to be approximately 100 MPa. A similar interpretation of impact events has been utilized for modeling and analysis of bird strikes on aerospace surfaces.[10] The orientation of the fruit fly at the impact event was considered to be inconsequential with respect to the dynamics. This was due to the impact velocities being greater than the rupture velocity (30 m s^{-1}) and orientation threshold velocity (55 m s^{-1}), defined as the velocity above which orientation does not influence residue properties.[11]

Fruit Fly Impacts on Al 2024 T3 clad

To ascertain the effect of impact angle, and build on previous studies,[11] fruit flies were impacted on cleaned Al alloy surfaces oriented at angles from 30-90°, where 90° was normal orientation to the airflow. Both impact dynamics and resultant residue properties were influenced by the impact angle, Fig. 1 and Table 1. For some impact events, especially those involving head or tail-first impact, portions of the insect exoskeleton remote from the actual contact point were observed to rupture (Fig. 1B at 90°). This behavior is consistent with hydrodynamic forces during high velocity impact of an incompressible fluid. Lamella formation was also observed, most notably at impact angles between 50-70°, (Fig. 1B and C at 60°), followed by fragmentation of the lamella or splashing, as it is referred to when discussing liquid droplet impact events. For all surfaces, initial impact resulted in an expansion of haemolymph with instability causing fingering as well as splashing.[12] For fingers that contacted the surface, the residues were observed to remain where initial contact was made without any noticeable retraction, even on μs timescales. This suggested that haemolymph viscosity had already significantly increased as a result of coagulation. At low impact angles, interactions with the surface resulted in more shearing phenomena instead of the compressive behavior observed at greater impact angles. This yielded a dramatically increased wetted area in the airflow direction relative to the span and significantly fewer large residues on the surface. Exoskeleton fragments were observed to tumble across the surface or slightly above the surface, ultimately becoming entrained in the airflow and removed from the surface.

Interestingly, the insect residue area reached a maximum at 70°. One possible explanation is that residue splashing occurred to a greater extent at impact angles > 70°, arising from rapid elastic rebound of haemolymph which would propel it outside of the stagnation layer at the impact site. Thus, splashing arising from lamella destabilization yielded residues that became entrained in airflow directed away from the impact site. At impact angles < 70°, the forces acting at the impact site were not symmetric which resulted in a reduced area of lamella propagation. Although not as distinct, residue height also appeared to decrease at impact angles < 70°.

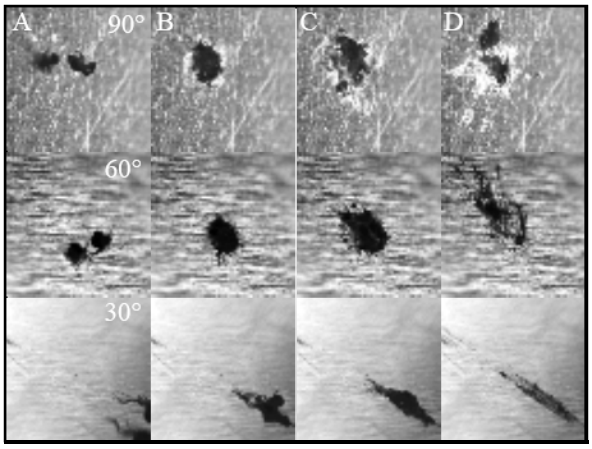

Figure 1. Fruit fly impact images on Al 2024 substrates at angles relative to the airflow as indicated in the figure. The images depict impact dynamics at (A) -10 μs, (B) 30 μs, (C) 50 μs, and (D) 1 ms after impact. For size reference, fruit flies are approximately 1 mm × 3 mm.

Table 1. Insect residue height and areal coverage results from fruit fly impact experiments on Al 2024 surfaces.

Impact Angle	Residue Height, μm	Residue Area, mm²
Airfoil	227±58	2.1±0.7
90	243±41	1.5±0.3
80	195±50	2.7±0.4
70	259±2	4.7±2.7
60	235±39	2.1±0.3
50	142±0.8	1.9±1.1
40	167±61	1.2±0.3
30	96±76	0.7±0.2

Fruit Fly Impacts on Research Coatings

Although it was previously reported that surface energy and topography were important factors in mitigation of insect residue adhesion, the effect of these factors on impact dynamics was not investigated. Therefore, several coatings were subjected to fruit fly impacts at a 60° impact angle (Fig. 2 and Table 2). This angle was selected to enable comparison with previous data collected on an airfoil shape that had given similar insect residue height and area coverage values (Table 1). Insect impacts on commercial urethane (CU) and research urethane (RU) surfaces resulted in similar impact characteristics and resultant residue properties, both of which were reduced relative to the control Al 2024 surface. Similarly, impacts on the research epoxy I (REI) surface resulted in impact dynamics similar to those observed on the urethane surfaces, i.e., initial lamella formation with expansion followed by fragmentation. The influence of surface roughness on lamella expansion and splashing was previously related qualitatively to a surface roughness parameter, S_a, calculated by dividing the roughness, R_a, by the droplet diameter, D.[12] For these surfaces, $S_a \ll 1$, so the wetting and ultimate residue properties would be dominated by surface chemistry.

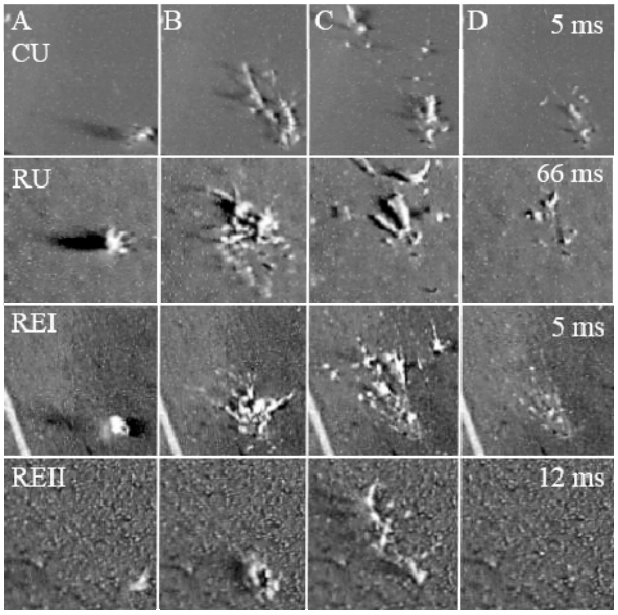

Figure 2. Fruit fly impact images on coated surfaces oriented at 60° relative to the airflow. The images depict the impact dynamics at (A) -10 μs, (B) 100 μs, (C) 300 μs, and (D) long times, as indicated, after impact. For size reference, fruit flies are approximately 1 mm × 3 mm.

Table 2. Surface and insect residue characterization from fruit fly 60° impact angle experiments.

Surface	θ_A, °	R_a, μm	Residue Height, μm	Residue Area, mm^2
Al 2024 Control	84±1	0.31	235±39	2.1±0.3
Commercial Urethane, CU	85±1	0.32	181±72	0.9±0.5
Research Urethane, RU	108±2	1.84	172±57	0.7±0.5
Research Epoxy I, REI	107±1	0.48	172±60	0.2±0.1
Research Epoxy II, REII	98±1	8.19	67±25	0.08±0.05

For all surfaces, the reduction in residue area arose from an increased instability in the lamella generated from the haemolymph observed shortly after impact. This instability was most obvious on the REII surface, where nominal lamella expansion leading to rapid splashing was observed (see frame B of REII in Fig. 2). The S_a value for this surface was nearly five times greater than values for the others. As can be seen, the residues appear to be concentrated and ejected from the surface earlier, relative to the other coatings. Due to the earlier onset of splashing, the residues were entrained in the airflow and removed from the surface to a greater extent, yielding lower residue height. Similarly, reduced wettability resulted in limited lamella expansion which decreased residue areal coverage. Both of these behaviors improved insect residue adhesion mitigation.

Conclusions

In these experiments, the effects of impact angle, surface energy, and topography on impact dynamics shortly after the impact event were investigated. Results suggest that the behavior of the lamella generated from the haemolymph needs to be considered to improve the performance of a surface designed for insect adhesion mitigation. Lamella behavior was influenced by the impact angle resulting in changes to the contact area upon impact. Both reduction in lamella expansion and stability, arising from surface chemical and topographical properties, reduced the amount of residues remaining on a surface.

Acknowledgements

The authors would like to thank Paul Bagby, NASA Langley Research Center, for collection of high-speed photography.

References

1. (a) R. Joslin, *Ann. Rev. Fluid Mech.* **1998,** 30, pp 1-29; (b) R. Joslin, Overview of Laminar Flow Control. National Aeronautics and Space Administration, 1998, NASA/TP-1998-208705.
2. T.R. Thompson, et al., Technology Portfolio Analysis for Environmentally Responsible Aviation. In *AIAA Aviation*, Atlanta, GA, 2014.
3. (a) G.V. Lachman, Aspects of Insect Contamination in Relation to Laminar Flow Aircraft. 1960, A.R. C. Technical Report, C.P. No. 484. (b) C.C. Croom and B.J. Holmes In *Insect Contamination Protection for Laminar Flow Surfaces*, Langley Symposium on Aerodynamics, Hampton, VA, Hampton, VA, 1986; pp 539-556. (c) M. Kok, et al., *Prog. Aerospace Sci.* **2014,** in press. (d) T. Young and B. Humphreys, *Proc. Instn. Mech. Engrs. G. J. Aerospace Eng.* **2004,** 218, pp 267-277.
4. M. Kok, et al., *Prog. Org. Coat.* **2013,** 76, pp 1567-1575.
5. (a) C.J. Wohl, et al., Polyimide-based Particulate Composite Coatings for Contamination Mitigation of Aircraft Surfaces. In *36th Annual Meeting of The Adhesion Society*, Daytona Beach, FL, 2013; (b) C.J. Wohl, et al., Novel Epoxy Particulate Composites for Mitigation of Insect Residue Adhesion on Future Aircraft Surfaces. In *37th Annual Meeting of the Adhesion Society*, San Diego, CA, 2014.
6. W.S. Coleman, Roughness Due to Insects. In *Boundary Layer and Flow Control: Its Principles and Applications*, Lachman, G. V., Ed. Pergamon Press: Oxford, 1961; pp 682-747.
7. J.S. Wilbeck, Impact Behavior of Low Strength Projectiles. Air Force, 1977, ADA060423.
8. M. Rein, *Fluid Dynamics Res.* **1993,** 12, pp 61-93.
9. C.J. Wohl, et al., *Prog. Org. Coat.* **2013,** 76, pp 42-50.
10. (a) M.N. Ensan, et al., *Trans. Canadian Soc. Mech. Eng.* **2008,** 32, pp 283-296. (b) S. Heimbs and T. Bergmann, *Int. J. Aerospace Eng.* **2012,** 2012, p 372167.
11. M. Kok, et al., *Aerospace Sci. Technol.* **2014,** in press.
12. C. Mundo, et al., *Int. J. Multiphase Flow* **1995,** 21, pp 151-173.